Supplementary Information

Symmetry analysis for magnetic structure determination

A symmetry analysis was performed using Bertaut's method[1] as implemented in the BasIReps program from the FullProf suite[2], in order to determine all of the possible spin configurations that are compatible with the crystal symmetry of $KFeSO_4F$ and the propagation vector $\mathbf{k}$ = (1, 0, 0). The little group $G_{\mathbf{k}}$ coincides with the full G = *C*2/*c* space group because all symmetry operators of G leave invariant (up to a reciprocal lattice vector) the propagation vector $\mathbf{k}$ = (1, 0, 0). There are four irreducible representations associated with the 8*f* and 4*e* Wyckoff sites occupied by iron atoms:

$\Gamma_{mag}(8f) = 3\,\Gamma_1 \oplus 3\,\Gamma_2 \oplus 3\,\Gamma_3 \oplus 3\,\Gamma_4$

$\Gamma_{mag}(4e) = \Gamma_1 \oplus \Gamma_2 \oplus 2\,\Gamma_3 \oplus 2\,\Gamma_4$

For the 8f site (Fe1), each representation is composed of three basis vectors Ψ_i (i=1, 2, 3) which correspond to moments oriented along the *a*, *b* or *c* unit-cell directions as given in Table 1. For Fe2 and Fe3 atoms (4*f* Wyckoff site), symmetry analysis imposes magnetic moments along [010] for representations Γ_1 and Γ_2, and perpendicular to [010] for Γ_3 and Γ_4.

The magnetic moments in the crystal can be obtained from the magnetic moments of the sublattice *j* (= 1, 2) in the zero-cell with the expression:

$$\mathbf{m}_{lj} = \mathbf{m}_{0j} \exp\{-2\pi i\, \mathbf{k}\, \mathbf{R}_l\} = \mathbf{m}_{0j} \exp\{-2\pi i\, (1\mathbf{a}^*).(\, l_1\, \mathbf{a} + l_2\, \mathbf{b} + l_3\, \mathbf{c})\, \} = \mathbf{m}_{0j} \exp\{-2\pi i\, l_1\}$$

where the lattice translation $\mathbf{R}_l = l_1\, \mathbf{a} + l_2\, \mathbf{b} + l_3\, \mathbf{c}$ contains integer values as well as rational values due to the centering translation $\mathbf{t}_C$ = (1/2, 1/2, 0), for instance the (1/2, 1/2, 0)+ set of atoms in the conventional cell have their moment opposite to those of the zero cell because $\exp(-2\pi i\, l_1) = \exp(-2\pi i\, .\, 1/2) = -1$.

(1) E. F. Bertaut, *J. Phys. Colloq.* 1971, **32** (C1), C1–C462 – C1–C470.

(2) J. Rodríguez-Carvajal, J. González Platas, *Fourier Program*.

SI Table 1:

Results of the symmetry analysis of the *C*2/*c* unit cell for the propagation vector **k** = (1, 0, 0). The characters (**χ**) of the representations and the basis vectors $\mathbf{\Psi}_i$ (i = 1, 2, 3), as well as the Fourier coefficients ($\mathbf{S_k} = \mathbf{m}$, magnetic moments) of the positions generated for the 8*f* (*x*, *y*, *z*) and 4*e* (0, y, ¼) Wyckoff sites are given for each irreducible representation Γ_n ($1 \leq j \leq 4$). Note that atoms linked to the (½, ½, 0)+ centering have opposite magnetic moments to those of the (0, 0, 0)+ lattice.

k = (1, 0, 0)							
		Fe1 in 8*f*				**Fe2 and Fe3 in 4*e***	
		Fe1(1)	**Fe1(2)**	**Fe1(3)**	**Fe1(4)**	**Fe2,3(1)**	**Fe2,3(2)**
		x, y, z	***-x, y, -z+½***	***-x, -y, -z***	***x, -y, z+½***	***0, y, ¼***	***0, -y, ¾***
Γ_1 *C*2/*c*	**χ**	1	1	1	1	1	1
	Ψ_1	1, 0, 0	$\bar{1}$, 0, 0	1, 0, 0	$\bar{1}$, 0, 0	0, 1, 0	0, 1, 0
	Ψ_2	0, 1, 0	0, 1, 0	0, 1, 0	0, 1, 0		
	Ψ_3	0, 0, 1	0, 0, $\bar{1}$	0, 0, 1	0, 0, $\bar{1}$		
	S_k	***M_X, M_Y, M_Z***	***-M_X, M_Y, -M_Z***	***M_X, M_Y, M_Z***	***-M_X, M_Y, -M_Z***	***0, M_Y, 0***	***0, M_Y, 0***
Γ_2 *C*2/*c*'	**χ**	1	1	-1	-1	1	-1
	Ψ_1	1, 0, 0	$\bar{1}$, 0, 0	$\bar{1}$, 0, 0	1, 0, 0	0, 1, 0	0, $\bar{1}$, 0
	Ψ_2	0, 1, 0	0, 1, 0	0, $\bar{1}$, 0	0, $\bar{1}$, 0		
	Ψ_3	0, 0, 1	0, 0, $\bar{1}$	0, 0, $\bar{1}$	0, 0, 1		
	S_k	***M_X, M_Y, M_Z***	***-M_X, M_Y, -M_Z***	***-M_X, -M_Y, -M_Z***	***M_X, -M_Y, M_Z***	***0, M_Y, 0***	***0, -M_Y, 0***
Γ_3 *C*2'/*c*'	**χ**	1	-1	1	-1	1	1
	Ψ_1	1, 0, 0	1, 0, 0	1, 0, 0	1, 0, 0	1, 0, 0	1, 0, 0
	Ψ_2	0, 1, 0	0, $\bar{1}$, 0	0, 1, 0	0, $\bar{1}$, 0	0, 0, 1	0, 0, 1
	Ψ_3	0, 0, 1	0, 0, 1	0, 0, 1	0, 0, 1		
	S_k	***M_X, M_Y, M_Z***	***M_X, -M_Y, M_Z***	***M_X, M_Y, M_Z***	***M_X, -M_Y, M_Z***	***M_X, 0, M_Z***	***M_X, 0, M_Z***
Γ_4 *C*2'/*c*	**χ**	1	-1	-1	1	1	-1
	Ψ_1	1, 0, 0	1, 0, 0	$\bar{1}$, 0, 0	$\bar{1}$, 0, 0	1, 0, 0	$\bar{1}$, 0, 0
	Ψ_2	0, 1, 0	0, $\bar{1}$, 0	0, $\bar{1}$, 0	0, 1, 0	0, 0, 1	0, 0, $\bar{1}$
	Ψ_3	0, 0, 1	0, 0, 1	0, 0, $\bar{1}$	0, 0, $\bar{1}$		
	S_k	***M_X, M_Y, M_Z***	***M_X, -M_Y, M_Z***	***-M_X, -M_Y, -M_Z***	***-M_X, M_Y, -M_Z***	***M_X, 0, M_Z***	***-M_X, 0, -M_Z***

SI Table 2:

Result of EDX measurements averaged over five different zones of a monoclinic $KFeSO_4F$ sample.

Element	**at%**
K	13.4(2)
Fe	11.8(1)
S	13.6(1)
O	51.9(3)
F	9.0(1)

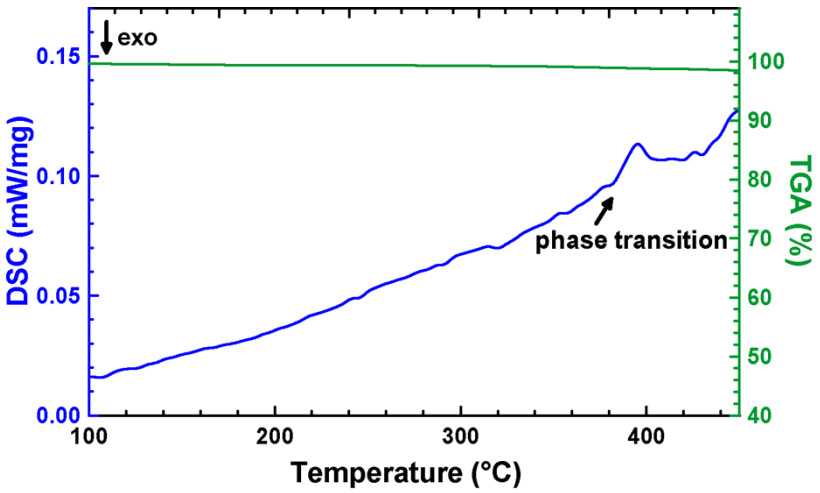

Figure SI 1: DSC measurement (blue) of the monoclinic $KFeSO_4F$ heated to 450 °C with a ramp of 1 °C/min under argon atmosphere. The onset of the monoclinic-orthorhombic phase transition is at 380°C. The green line corresponds to a coupled TGA measurement.

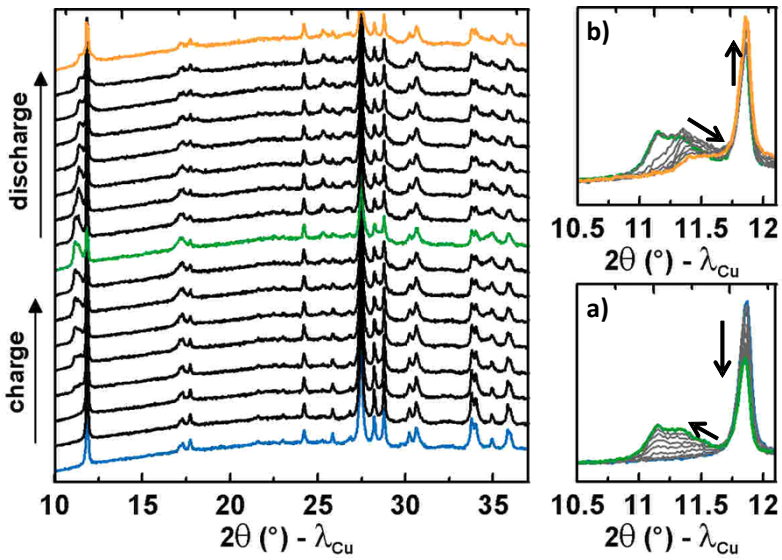

Figure SI 2: *In situ* XRD patterns of the pristine monoclinic $KFeSO_4F$ during the charge (K extracted) and subsequent discharge (Li inserted) indicative of a reversible biphasic process. Zoom at the evolution of the (002) peak during a) charge and b) discharge.

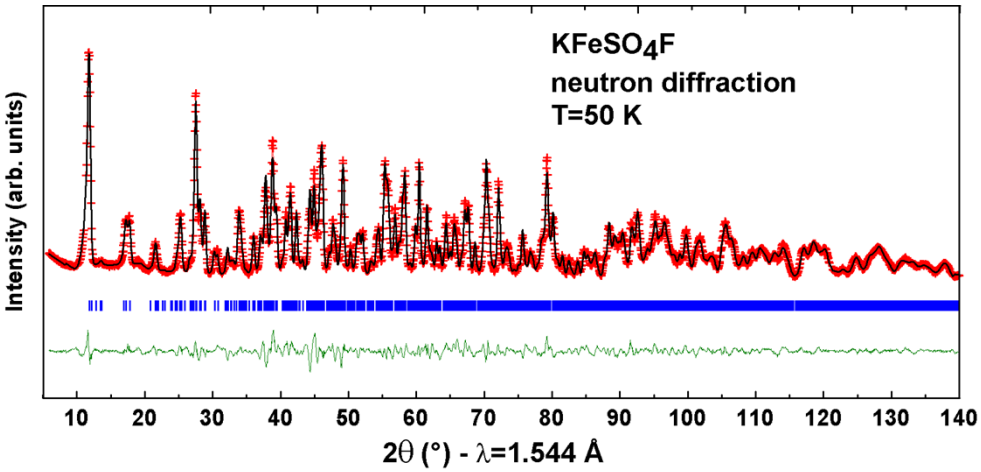

Figure SI 3: Rietveld refinement of and neutron powder diffraction patterns of $KFeSO_4F$ at T=50 K. The red crosses, black continuous line and bottom green line represent the observed, calculated, and difference patterns, respectively. Vertical blue tick bars are the Bragg positions for space group *C*2/*c*.